

Photography in the ultraviolet and visible violet spectra: Unravelling methods and applications in palaeontology

GAIA CRIPPA and STEFANO MASINI



Crippa, G. and Masini, S. 2022. Photography in the ultraviolet and visible violet spectra: Unravelling methods and applications in palaeontology. *Acta Palaeontologica Polonica* 67 (3): 685–702.

We have tested different preparation and photographic methods to define a protocol for UV analysis of fossil specimens. We also have explored its main applications while analysing specimens from different stratigraphic contexts, of different biomineralogical composition, and belonging to different fossil groups (including invertebrates and vertebrates). We have photographed specimens using a camera equipped with appropriate lens and filters both in visible light and with flashlights at two wavelengths: the 365 nm UV light and the 440 nm visible violet spectrum, the latter here tested for the first time. Our results indicate that bleach treatment is not recommended for calcite-shelled brachiopods, while it is suggested for aragonite-shelled molluscs. We show that photography in the ultraviolet and visible violet spectra are useful tools enhancing the recognition of morphological characters and colour patterns and allowing to distinguish soft-bodied fossils from the matrix. Also, it allows to discern specimen areas embedded in the sediment from those exposed to sunlight, which is helpful to reconstruct the conditions experienced by fossils. However, the mineralogy of the biomineral affects UV responses, as morphological characters of calcite shells are better emphasized with the 440 nm wavelength (visible violet spectrum), whereas those of aragonite, bioapatite and phosphatized specimens with the 365 nm (ultraviolet spectrum); also, shell microstructures with their different crystal arrangement and elemental incorporation may cause different reactions, whereas the stratigraphic context affects specimen preservation influencing pigment preservation. We thus provide a protocol for photography in the ultraviolet and visible violet spectra and show that this technique has a high potential in palaeontology, having no limitations for its application in invertebrate or vertebrate specimens.

Key words: Biominerals, fossil specimens, shell colour pattern, UV photography, visible violet spectrum.

Gaia Crippa [gaia.crippa@unimi.it] and Stefano Masini [stefano.masini92@gmail.com], Dipartimento di Scienze della Terra “A. Desio”, Università degli Studi di Milano, via Mangiagalli 34, Milano, 20133, Italy.

Received 29 September 2021, accepted 2 May 2022, available online 29 August 2022.

Copyright © 2022 G. Crippa and S. Masini. This is an open-access article distributed under the terms of the Creative Commons Attribution License (for details please see <http://creativecommons.org/licenses/by/4.0/>), which permits unrestricted use, distribution, and reproduction in any medium, provided the original author and source are credited.

Introduction

The analysis of fossil specimens with ultraviolet (UV) photography represents a helpful tool to be used in palaeontology which has been frequently applied in this field only in the last twenty years, although it was discovered at the beginning of the 20th century (see Tischlinger and Arratia 2013). In being a non-destructive method for fossil specimens it is a part of the palaeometric analysis (Riquelme et al. 2009). Up to now UV photography has been mainly applied to mollusc shells, but the number of studies dealing with other taxa, like vertebrate specimens (e.g., reptiles, fishes), is increasing (e.g., Haug et al. 2009; Hone et al. 2010, 2012; Lindgren et al. 2010; Tischlinger and Arratia 2013 and reference therein; Crippa and Teruzzi 2017).

Despite this, the analysis of fossil specimens under UV light represents a technique still not fully comprehended; the knowledge of the best procedure of sample preparation

and photography still needs to be clarified and new data are required to better understand the real potential of this method (see Tables 1, 2 for the state of the art on the different UV methodologies used in the literature).

Ultraviolet light in palaeontology has been mainly applied for systematic purposes, as this technique allows to better highlight morphological characters and, in the case of molluscs, also shell colour patterns (e.g., Olsson 1967; Vokes and Vokes 1968; Pitt and Pitt 1993; Merle et al. 2008; Hone et al. 2010, 2012; Lindgren et al. 2010; Caze et al. 2011a, b, 2012, 2015; Koskeridou and Thivaïou 2012; Tischlinger and Arratia 2013; Hendricks 2015). As observed by several authors (e.g., Caze et al. 2012; Hendricks 2015), many modern gastropod shells show distinctive colour patterns, which often constitute a decisive criterion for distinguishing and characterising biological groups and species (e.g., Conidae; Hoerle 1976; Hendricks 2015, 2018). In the fossil record, these colour patterns are rarely observable in visible light,

Table 1. Different treatments used for preparing fossil and modern specimens to UV photography.

Taxa analysed and reference	Treatment	Time of exposure
Fossil (Cenozoic) and modern Gastropoda from Florida, USA (Krueger 1974)	bleach	72 h
Muricidae (Gastropoda) from the Paleogene of the Paris Basin, France (Merle 2003)	no treatment	
Helicoidea (Gastropoda) from the Middle Miocene of Poland (Górka 2008)	no treatment	
<i>Vicarya</i> (Gastropoda) from the Lower–Middle Miocene of Japan and SE Asia (Kase et al. 2008)	shells soaked in commercially diluted chlorine laundry bleaching solution (“Kitchin Heiter”, chlorine-type, Kao Co. Ltd.) for 1–3 days	24–72 h
Bivalves and gastropods from the Eocene of the Paris Basin, France (Merle et al. 2008)	shells bathed in concentrated bleach for 24 h, then washed to eliminate traces of bleach	24 h
Crustaceans from the Upper Jurassic of Germany and the Upper Cretaceous of Lebanon (Haug et al. 2009)	no treatment	
<i>Microraptor gui</i> (Theropoda) from the Lower Cretaceous of China (Hone et al. 2010); pterosaur from the Upper Jurassic of Solnhofen, Germany (Hone et al. 2012)	no treatment	
Ampullinidae (Gastropoda) from the Mesozoic and the Cenozoic of France (Caze et al. 2011a); bivalves and gastropods from Eocene of the Paris Basin, France (Caze et al. 2012)	shells bathed in concentrated bleach, then carefully washed with water to eliminate all traces of dried sodium hypochlorite	24 h
<i>Glycymeris</i> (Bivalvia) from the Pliocene of Greece and the Eocene of France (Koskeridou and Thivaïou 2012)	shells bathed in sodium hypochlorite for 24 h, washed in water for 7 days and dried to avoid the formation of sodium deposits on the surface of the shells	24 h
Fossil bivalves and gastropods from the Jurassic of France (Caze et al. 2015)	shells immersed in a concentrated sodium hypochlorite solution (9.6% chlorine) for 24 h; many fragile aragonitic shells glued previously	24 h
Conidae (Gastropoda) from the Neogene of Dominican Republic (Hendricks 2015)	specimens scrubbed under water to remove attached sediments; then soaked overnight in a solution of diluted (50%) Clorox bleach and rinsed again in water and dried	12 h
Invertebrate and vertebrate specimens from different stratigraphic contexts (Crippa and Teruzzi 2017)	no treatment	
Brachiopods from the Cambrian of USA (Gaspard et al. 2019), from the Triassic and the Upper Cretaceous of France (Gaspard and Loubry 2017; Gaspard et al. 2019); modern brachiopods from the Japan coast, New Zealand, Caribbean Sea, Atlantic and Pacific Ocean (Gaspard et al. 2019)	no treatment in bleach (to avoid alteration/destruction of organic matrix within the biomineral)	

but they may become clear when fossil shells are viewed under UV light, which causes formerly pigmented regions of the shell to fluoresce (e.g., Krueger 1974; Caze et al. 2015; Hendricks 2015). In fact, according to Krueger (1974), what a shell exhibits under UV light is the colour pattern or the region once pigmented, but not the original colour. Since the discovery that colour ornamentations in mollusc shells may be revealed and emit fluorescence under UV light many researchers started to explore this technique (see Caze et al. 2012 and Tischlinger and Arratia 2013 for an overview on UV light imaging history). In particular, as the cause of the fluorescence may reside into shell pigments, several papers investigated the chemical nature of the pigment, and thus the source of the colour, mainly using Raman spectroscopy (e.g., Comfort 1951; Barnard and de Waal 2006; Hedegaard et al. 2006; Gaspard et al. 2019). However, pigments are difficult to extract from the shell and thus to identify, so their knowledge remains limited and uncompleted. An extensive discussion on mollusc pigments and on their possible functions has been provided by Caze et al. (2012) and Williams (2017).

There is still no clear understanding of exactly what chemical compounds are responsible for pigmentation in modern shells, and much less is known of what actually fluoresces in the fossil shells (Hendricks 2015). The preservation of the colour pattern in fossil specimens is considered an exceptional phenomenon due to the fast degradation of pigments after the death of the organism and during the fossilization process; exceptional conditions are needed to preserve the shell colour, as a rapid burial to protect the pigments from the decomposition by microorganisms or from sun ultraviolet radiation (e.g., Caze et al. 2012; Williams 2017). Generally, only a few remarkably well-preserved specimens display remnants of colour pattern (Caze et al. 2012). However, when preserved, the identification of residual colour ornamentations under UV light in fossil specimens may be of great help in discriminating between different species and in understanding the systematic of some fossil molluscs.

Residual colour pattern is not the only character which can be revealed observing fossil specimens under UV light.

Table 2. Photographic techniques and UV wavelengths used in different studies.

Reference	UV wavelength	Photographic procedure
Krueger 1974	no data	A modern shell and a fossil relative were photographed together under white light and UV light. A standard medium yellow filter was used over the lens to eliminate the reflected UV light and admit only the fluorescent lights into the camera.
Merle 2003	360 nm	no data
Górka 2008	UV-A	Shells were analysed in daylight and under UV-light. The source of UV-light was a standard Wood's mercury UV-A lamp (EMITAVP-60).
Kase et al. 2008	254/365 nm	Shells were photographed using a Nikon D70s digital camera equipped with a Micro Nikkor AF lens (60 mm, 2.8D) with two filters (Kodak CC30R and Wratten no. 2E) under handy UV lamps (SLUV-8, 254/365 nm, As One Co. Ltd.). Pictures were processed using Adobe Photoshop 6.0, inverted, greyscaled, and adjusted in brightness, contrast, etc.
Merle et al. 2008	360 nm	no data
Haug et al. 2009	358 nm	Several overlapping images of the complete specimen were combined partially automated using the photomerge function and/or by hand in Photoshop and GIMP. Photos were taken under (i) normal light using a Leica stereomicroscope with a mounted DCM 500 ocular camera using a ring lamp; the camera was set to take an image every two seconds, while the focus was progressively shifted manually; (ii) ultraviolet light (358 nm, Axio Scope 2 with a mounted AxioCam); (iii) green light (546 nm).
Hone et al. 2010, 2012	365–366 nm	Different color filters (yellows, blues and reds of different types and densities and in different combinations) were affixed to the camera or microscope lens for a selective visualisation of peculiar fine structures by providing additional contrast. The first filter is a UV Filter supposed to block UV light up to 390 nanometers (e.g., Hama or Hoya brand O-Haze).
Caze et al. 2011a, 2012	360 nm	Specimens were placed at the intersection of the beams of two UV lamps arranged face to face and emitting the same wavelength. To get the best images software processing (brightness and contrast adjustment) were used. The photographed specimens are presented as imaged under UV light and not in negative view.
Koskeridou and Thivaïou 2016	360 nm	no data
Caze et al. 2015	360 nm	no data
Hendricks 2015	365 nm	Specimens were photographed using either a Canon 50D or Nikon 7100D digital camera attached to a copy stand. Two Raytech LS-7CB lamps were used for UV photography in a dark room or a large box was used to cover the entire photography apparatus. Figures were prepared using Adobe Photoshop CS6. Adjustments were made to the white balance and levels of individual images, and treated using the auto tone, auto contrast, and/or auto color functions of Photoshop. Most UV light images were digitally reversed (using Photoshop's invert function) to reconstruct shell coloration patterns.
Crippa and Teruzzi 2017	365 nm	Specimens were photographed with a digital camera mounted on a photographic stand in a dark room. Four fixed Wood's lamp were used together with a portable flashlight, both emitting a 365 nm wavelength.
Gaspard and Loubry 2017; Gaspard et al. 2019	360 nm	Modern species displaying a colouration were illustrated under daylight. Shells were observed, without filters, using the classical support of photography in natural light (3 lamps Dedo-light DLH4 (Halogen 24 V/150 W) + diffusers). Fossil species were illustrated alike and with UV light using two UV lamps Fluotest Forte (230V, 50Hz, 210W) emitting at a wavelength of 360 nm in a dark room.

This technique allows to improve the visualization of specimens that are, in visible light, difficult to distinguish in colour or texture from the surrounding matrix, providing greater clarity of some details and visualization of soft anatomical tissues (Crippa and Teruzzi 2017; Eklund et al. 2018). Indeed, the observation of vertebrate specimens under UV light allows the identification of soft tissues and other features that are difficult or impossible to see in visible light, like feathers, cartilage, skin, scales, membranes or tooth wear, as it has been shown by Hone et al. (2010) in the theropod dinosaur *Microraptor gui* or by Tischlinger and Arratia (2013) in Mesozoic fishes. Besides being very useful for systematic aims, this approach represents also an important aid during the preparation of fossil specimens (Haug et al. 2009; Hone et al. 2010, 2012). Calcite-shelled brachiopods in particular are interesting as until now many studies employing UV light have been performed on molluscs, ar-

thropods or vertebrate specimens, but very few dealt with brachiopods (Gaspard and Loubry 2017; Gaspard et al. 2019 and reference therein), which however are among the most common macroinvertebrate taxa in the fossil record (Harper et al. 2017). For these reasons, here we choose to investigate also species of this phylum.

Finally, the use of UV light provides an inexpensive method to detect, record, and understand some man-made interventions in fossil specimens and thus retouched fossils (e.g., Corbacho and Sendino 2012; Tischlinger and Arratia 2013; Crippa and Teruzzi 2017; Eklund et al. 2018).

The procedures to prepare specimens for UV photography are varied (Table 1). For instance, papers dealing mainly with fossil mollusc shells have shown that the residual colour pattern may be revealed or enhanced by bleaching specimens in sodium hypochlorite (NaClO) rather than by directly exposing them under UV light (e.g., Krueger 1974;

Kase et al. 2008; Merle et al. 2008; Caze et al. 2011a, 2012, 2015; Hendricks 2015). According to Caze et al. (2012), bleach oxidises pigment residuals, invisible in visible light, making them to fluoresce under UV light.

Here, we test different preparation techniques for fossil brachiopod and mollusc specimens, using, as a starting point, methods previously described in the literature (see Table 1), varying bleach concentrations and times of exposure to establish a protocol which can represent a benchmark for future studies. Subsequently, we photograph specimens first in visible light, then using two different wavelengths: the commonly used 365 nm UV light, and the 440 nm, here adopted for the first time; the latter does not properly belong to the ultraviolet spectrum but to the visible violet (hereinafter VV). Furthermore, we test the response, under these two wavelengths, of vertebrate and invertebrate taxa with different biominerals (brachiopods, bivalves, gastropods, crustaceans, fishes, and reptiles), not treated with bleach, but photographed using the same abovementioned procedure. With this contribution we aim to define a protocol for photography in the ultraviolet and visible violet light spectra of fossil specimens and to show the best results of the application of this technique to different taxa coming from different stratigraphic and geographic contexts (from the Permian to the Holocene, from Oman to Italy) and having different biominerals.

Institutional abbreviations.—MCSNIO, Museo Civico di Scienze Naturali di Induno Olona, Italy; MPUM, Museo di Paleontologia dell'Università di Milano, Italy.

Other abbreviations.—UV, ultraviolet; VV, visible violet.

Material

The analyses here presented have been performed on specimens from different fossil groups (brachiopods, bivalves, gastropods, crustaceans, fishes, and reptiles) from different stratigraphic contexts (Permian, Triassic, Cretaceous, Pleistocene, and Holocene) and having different biominerals (low magnesium calcite, aragonite, bioapatite, and phosphatized and silicified specimens). This choice has been made in order to test the different applications of UV and VV photography in palaeontology analysing the widest conditions as possible.

Sixteen macroinvertebrates specimens, belonging to different species of brachiopods, bivalves and gastropods, have been specifically selected to test treatments with commercial bleach. These include four specimens of brachiopods, eight bivalves and four gastropods.

Brachiopods belong to the spiriferinid *Pachycyrtella omanensis* Angiolini, 2001, from the lower Permian Saiwan Formation (285 Ma) in Oman; two ventral valves MPUM 12152 (#55), MPUM 12153 (OL130A); one dorsal valve MPUM 12151 (#38); one articulated specimen MPUM

12154 (OL130B). Specimens have been collected from the 60 cm-thick *Pachycyrtella* Bed, which records a cold-water palaeocommunity living in eutrophic conditions on mobile arenitic substrates in shallow water (Angiolini 2007). The *P. omanensis* specimens have experienced no or a very limited post-mortem transportation; indeed, they show an excellent preservation suggesting a fast burial (Angiolini 2007).

Bivalves belong to the pectinid *Aequipeecten opercularis* (Linnaeus, 1758), MPUM 12155 (ACG194-5), MPUM 12160 (ACG222); the venerid *Chamelea gallina* (Linnaeus, 1758), MPUM 12156 (ACG259), MPUM 12161 (ACG204); and the arcoid *Glycymeris nummaria* (Linnaeus, 1758), MPUM 12157 (ACG204-A), MPUM 12159 (ACG204-4), MPUM 12158 (ACG261), MPUM 12162 (ACG261-1). They all have been collected from several sandy and silty beds of the Lower Pleistocene Arda River marine succession (Calabrian, 1.8–1.2 Ma) located near Castell'Arquato in northern Italy (Crippa et al. 2018). The marine succession corresponds to a subaqueous extension of a fluvial system affected by high-density flows triggered by river floods, with supposed water depths ranging between 5 and 50 m (Crippa et al. 2018, 2020a). Bivalves show an excellent preservation, often preserving the colour pattern ornamentation.

Gastropods belong to the olivid *Oliva bulbosa* (Röding, 1798), MPUM 12165 (BS-68), MPUM 12166 (BS-94) and the conid *Conus* sp., MPUM 12163 (BS-148), MPUM 12164 (BS-150). They come from the Inqitat Khor Rori Archaeological Park in Dhofar, southern Oman. These specimens are dated to the Meghalayan (Holocene), ca. between the IV century BC and the I–II century AD (Silvia Lischi, personal communication 2019) and have been collected from an anthropogenic shell accumulation within megalithic circular structures (Lischi 2016). The preservation of the specimens is generally good, retaining the original mineralogy and ornamentation, but showing often corrosion.

In addition, in order to test the response of fossil specimens under two different wavelengths (365 nm and 440 nm), we have analysed further samples with different biominerals and belonging to both vertebrate and invertebrate taxa (bivalve rudists, crustaceans, fishes, and reptiles), which have not been exposed to any particular treatment.

Rudists consist of a right valve belonging to the hippuritid *Vaccinites* sp., MPUM 12167 (OMAN-1) from the Campanian (Upper Cretaceous) Samhan Formation outcropping south of Saiwan (Oman) (Philip and Platel 1995; Simonpietri et al. 1998). The Samhan Formation deposited in a neritic shelf environment and it consists of detrital sandy or marly facies with rudist biostromes (Philip and Platel 1995). The specimens are silicified (Philip and Platel 1995; GC and SM, personal observations).

The marine reptile belongs to the sauropterygian *Lariosaurus valceresii* Tintori and Renesto, 1990, MCSNIO 701; the UV photos have been taken on the skull. The fish belongs to the actinopterygian *Prohalecites porroi* (Bellotti, 1857), MPUM 12169, and the crustacean to the lophogastrid *Vicluvia lombardoae* Larghi, Tintori, Basso, Danini,

Table 3. Collection numbers, species and valve analysed, and treatment type experienced by the specimens of brachiopods, bivalves, and gastropods here investigated.

Taxon	Specimen number	Species	Valve	Pure bleach		Diluted bleach	
				3/24/72h	72h	3/24/72h	72h
Brachiopoda	MPUM 12151 (#38)	<i>Pachycyrtella omanensis</i>	dorsal	×			
	MPUM 12152 (#55)	<i>Pachycyrtella omanensis</i>	ventral		×		
	MPUM 12153 (OL130A)	<i>Pachycyrtella omanensis</i>	ventral				×
	MPUM 12154 (OL130B)	<i>Pachycyrtella omanensis</i>	articulated			×	
Bivalvia	MPUM 12155 (ACG194-5)	<i>Aequipecten opercularis</i>	left	×			
	MPUM 12156 (ACG259)	<i>Chamelea gallina</i>	left		×		
	MPUM 12157 (ACG204-A)	<i>Glycymeris nummaria</i>	left		×		
	MPUM 12158 (ACG261)	<i>Glycymeris nummaria</i>	right		×		
	MPUM 12159 (ACG204-4)	<i>Glycymeris nummaria</i>	left				×
	MPUM 12160 (ACG222)	<i>Aequipecten opercularis</i>	right				×
	MPUM 12161 (ACG204)	<i>Chamelea gallina</i>	right			×	
	MPUM 12162 (ACG261-1)	<i>Glycymeris nummaria</i>	right			×	
Gastropoda	MPUM 12163 (BS-148)	<i>Conus</i> sp.			×		
	MPUM 12164 (BS-150)	<i>Conus</i> sp.		×			
	MPUM 12165 (BS-68)	<i>Oliva bulbosa</i>				×	
	MPUM 12166 (BS-94)	<i>Oliva bulbosa</i>					×

and Felber, 2020 (MPUM 12168), the latter showing phosphatization (Montagna et al. 2017; Larghi et al. 2020). All these specimens come from the Ladinian (Middle Triassic) Kalkschieferzone, the uppermost level of the Meride Limestone, consisting of well-bedded and/or laminated limestone and marly limestone, outcropping in the fossiliferous locality Cà del Frate (Viggiù, Lombardy, northern Italy) (Tintori 1990; Renesto et al. 2004; Larghi et al. 2020). The biota of the Kalkschieferzone lived in a tropical climate subjected to strong seasonal changes, recording mainly marine conditions with short intervals suggesting brackish and/or freshwater environments (Lombardo et al. 2012).

All the specimens here analysed are housed in the collections of the Dipartimento di Scienze della Terra “A. Desio” of the University of Milan (MPUM-numbers; Table 3) and the Museo Civico di Scienze Naturali, Induno Olona, Lombardy, Italy (MCSNIO-numbers).

Methods

Specimens preparation.—Specimens of brachiopods, bivalves and gastropods have been treated with commercial bleach (containing 3–5% of sodium hypochlorite) in order to oxidise, if present, pigment residuals, which are invisible in visible light, but may fluoresce under UV and VV light. We have tested different preparation techniques of fossil brachiopods and molluscs, varying bleach concentrations and the time of exposure (Table 3). Some specimens have been bathed in pure (i.e., not diluted) commercial bleach: *Pachycyrtella omanensis* MPUM 12151 (#38), MPUM 12152 (#55); *Aequipecten opercularis* MPUM 12155 (ACG194-5); *Chamelea gallina* MPUM 12156 (ACG259); *Glycymeris nummaria* MPUM 12157 (ACG204-A), MPUM 12158

(ACG261); *Conus* sp. MPUM 12163 (BS-148), MPUM 12164 (BS-150), whereas others in 50% diluted commercial bleach: *Pachycyrtella omanensis* MPUM 12153 (OL130A), MPUM 12154 (OL130B); *Aequipecten opercularis* MPUM 12160 (ACG222); *Chamelea gallina* MPUM 12161 (ACG204); *Glycymeris nummaria* MPUM 12159 (ACG204-4), MPUM 12162 (ACG261-1); *Oliva bulbosa* MPUM 12165 (BS-68), MPUM 12166 (BS-94). Pure means that the commercial bleach was not diluted. All the experiments have been performed at room temperature under an extractor fume hood. Also, we have tested different times of exposure to pure or diluted bleach photographing the specimens after 3, 24, and 72 hours respectively: *Pachycyrtella omanensis* MPUM 12151 (#38), MPUM 12154 (OL130B); *Aequipecten opercularis* MPUM 12155 (ACG194-5); *Chamelea gallina* MPUM 12161 (ACG204); *Glycymeris nummaria* MPUM 12162 (ACG261-1); *Conus* sp. MPUM 12164 (BS-150); *Oliva bulbosa* MPUM 12165 (BS-68) or directly after 72 h: *Pachycyrtella omanensis* MPUM 12152 (#55), MPUM 12153 (OL130A); *Aequipecten opercularis* MPUM 12160 (ACG222); *Chamelea gallina* MPUM 12156 (ACG259); *Glycymeris nummaria* MPUM 12159 (ACG204-4), MPUM 12157 (ACG204-A), MPUM 12158 (ACG261); *Conus* sp. MPUM 12163 (BS-148); *Oliva bulbosa* MPUM 12166 (BS-94).

All the specimens have been photographed before and after each treatment in pure or diluted bleach, first in visible light and then using two different wavelengths (365 nm and 440 nm). After each treatment in bleach and before being photographed the specimens have been rinsed in distilled water and air dried.

In addition, other specimens have been photographed without bleach treatment: *Vaccinites* sp., *Vicluvia lombardiae*, *Prohalecites porroi*, and *Lariosaurus valceresii*. These samples have been only photographed in UV and VV light with the procedure described in detail below.

Photographic procedure.—Photographs have been taken with a Samsung NX3300 mirrorless camera equipped with a Super-Paragon PMC 28 mm lens and mounted on a tripod with reclining arms; the camera focal axis has been kept orthogonal to the surface with samples. Images have been captured in the dark, as the fluorescence UV-induced is higher if the photographic set lacks visible light; each specimen has been placed on a black background (black cardboard). Before taking photos the specimens and the background have been carefully cleaned with compressed air in order to remove small particles of dust, which are highly reactive under UV light; brushes have proved to be ineffective. Finally, a scale and a white gypsum have been placed close to each specimen; the latter has been used to provide a reference for white balance during photo post-production.

The camera picks up a wavelength spectrum greater than the visible one (380–780 nm). Therefore, we have used a Hoya “UV + IR cut” filter to cut off the amount of ultraviolet and infrared wavelengths typically received by the camera. The ultraviolet light sources have been provided by two flashlights (KL 365 and KL 440, MADatec s.r.l.), which emit a focused light beam with a wavelength of 365 nm and 440 nm, respectively. The 440 nm wavelength induces a wide spectrum of fluorescence, which needs to be cleaned from the visible light component using a “B+W 52 022 2X MRC” yellow filter (MADatec s.r.l.). Regarding the camera settings we have used a ISO400 sensitivity, a F10 diaphragm aperture and a shutter speed of 1/10, 0.6–0.8 and 0.2–0.5, for photos taken in visible light, under 365 nm, and 440 nm, respectively.

Each specimen has been photographed first in visible light and then with 365 nm and 440 nm wavelengths keeping the camera and the specimen in the same positions during the photo capture with different wavelengths; then the same procedure has been repeated for the subsequent specimen. This allows an easier comparison between photos of the same specimen taken with different wavelengths. When taking UV and VV photographs, we have used protective glasses and gloves as personal safety.

Images have been saved in RAW format to preserve the maximum range of colour and light-intensity values that the sensor is capable of recording. Photo saving in JPEG or TIFF formats is discouraged, as these file types transform and balance automatically the colours in an irreversible way. The colours balance has been performed with the software “Samsung Raw Converter” using the white gypsum as reference. The resulting images have been then converted in JPEG format and the most significant ones are shown in Figs. 1–5.

Results

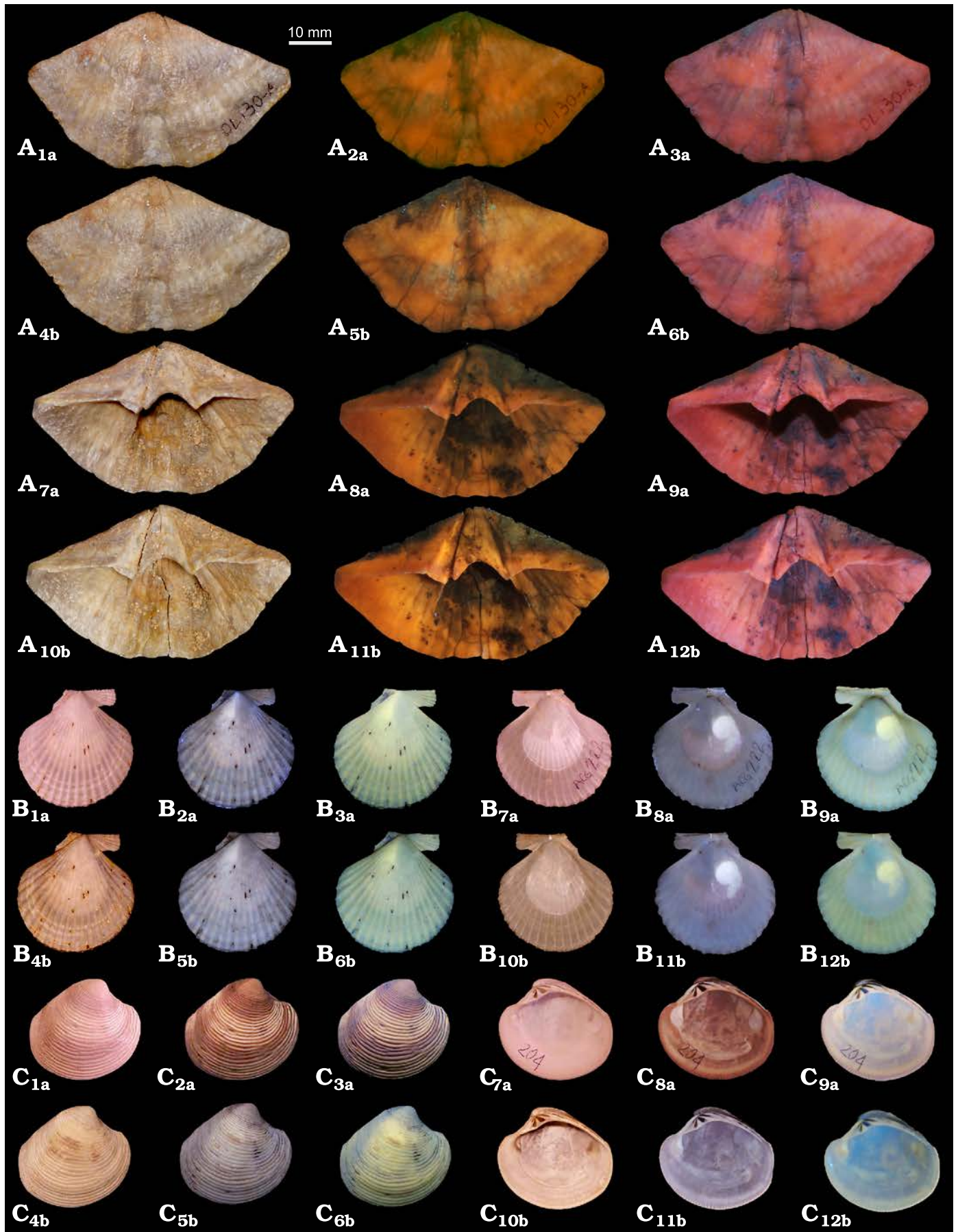
The results of photography in visible light and under 365 nm (UV) and 440 nm (VV) wavelengths of brachiopods, bivalves, and gastropods before and after the immersion in pure or diluted commercial bleach for 72 h are illustrated in Figs. 1–3; images of the specimens photographed after 3, 24, and 72 h are illustrated in the SOM: figs. S1–S4 (Supplementary Online Material available at http://app.pan.pl/SOM/app67-Crippa_Masini_SOM.pdf). No particular difference is observed among specimens treated with pure or diluted commercial bleach (Figs. 1–3; SOM: figs. S1–S5).

Morphological characters of the brachiopod shell (MPUM 12153 [OL130A], Fig. 1A; MPUM 12154 [OL130B], SOM: fig. S1), such as the ventral sulcus, the interarea and the muscle field, are better highlighted by the 440 nm wavelength (Fig. 1A_{3a}, A_{6b}, A_{9a}, A_{12b}) rather than by the 365 nm one (Fig. 1A_{2a}, A_{5b}, A_{8a}, A_{11b}), as the former wavelength results in brighter images. The encrusting sediment under UV and VV light assumes a dark colour allowing to distinguish it clearly from the shell; this distinction is not observable when the specimen is photographed in visible light (Fig. 1A_{1a}, A_{4b}, A_{7a}, A_{10b}). A 72 hours immersion of the specimen in diluted commercial bleach slightly enhances the luminescence of the shell when photographed in UV and VV light (Fig. 1A_{5b}, A_{6b}, A_{11b}, A_{12b}).

Contrary to brachiopods, morphological characters and colour patterns of both bivalves and gastropods seem to be better emphasized when photos are taken using the 365 nm wavelength rather than the 440 nm (Figs. 1B, C, 2).

The muscle scar in *Aequipecten opercularis* (MPUM 12160 [ACG222], Fig. 1B_{7a}–B_{9a}, B_{10b}–B_{12b}) is highlighted and emits a white-yellow fluorescence with both wavelengths; this is not the case for *Chamelea gallina* (MPUM 12161 [ACG204], Figs. 1C, 3A, SOM: fig. S2G–L), where the muscle scars are only slightly enhanced by UV light photographs. However, in both species the internal characters are clearer when the specimens are examined under UV and VV light rather than in visible light. Indeed, in *Chamelea gallina* the hinge teeth are more definite due to the presence of sediment within the sockets which under UV and VV light has a dark colour thus enhancing the contrast with the shell. Also, the external colour banding in *Chamelea gallina* is emphasized by UV and VV light (Fig. 1C_{2a}, C_{3a}, C_{5b}, C_{6b}) compared to visible light (Fig. 1C_{1a}, C_{4b}). The immersion in diluted commercial bleach for 72 h, besides whitening the shell, reveals a fine zig zag colour pattern in the middle-ventral part of the valve (Figs. 1C_{4b}–C_{6b}, 3A₂–A₄) which is not detectable in the shell before bleach treatment. A similar, but most prominent

Fig. 1. Brachiopods and bivalves photographed under visible, UV, and VV light. **A.** Spiriferinid brachiopod *Pachycyrtella omanensis* Angiolini, 2001, → from the lower Permian Saiwan Formation, Oman. MPUM 12153 (OL130A), ventral valve in external (A₁–A₆), and internal (A₇–A₁₂) views, visible light (A₁, A₄, A₇, A₁₀), 365 nm (A₂, A₅, A₈, A₁₁) and 440 nm (A₃, A₆, A₉, A₁₂). **B.** Pectinid bivalve *Aequipecten opercularis* (Linnaeus, 1758) from the Lower Pleistocene Arda River section, Italy. MPUM 12160 (ACG222), right valve in external (B₁–B₆) and internal (B₇–B₁₂) views, visible light (B₁, B₄, B₇, B₁₀), 365 nm (B₂, B₅, B₈, B₁₁) and 440 nm (B₃, B₆, B₉, B₁₂). **C.** Venerid bivalve *Chamelea gallina* (Linnaeus, 1758) from the Lower Pleistocene Arda River section, Italy. MPUM 12161 (ACG204), right valve in external (C₁–C₆) and internal (C₇–C₁₂) views, visible light (C₁, C₄, C₇, C₁₀), 365 nm (C₂, C₅, C₈, C₁₁) and 440 nm (C₃, C₆, C₉, C₁₂). a, without treatment; b, after 72 h of immersion in 50% diluted bleach.





result, is observable in the specimen of *Glycymeris nummaria* (MPUM 12157 [ACG204-A], Figs. 2C, 3B) after 72 h of immersion in pure commercial bleach: a well-defined colour pattern (red-orange) appears after the treatment; this is also evident in visible light but is enhanced by UV light, although it does not fluoresce (Figs. 2C_{4b}–C_{6b}, 3B₂–B₄). The muscle scars and the pallial line are fluorescent (white-yellow fluorescence) under UV and VV light, but faint in visible light (Fig. 2C_{7a}–C_{12b}). The hinge area with sediment among sockets is enhanced under UV and VV light.

Photographs under UV and VV light of the specimen of *Oliva bulbosa* (MPUM 12166 [BS-94], Fig. 2A; MPUM 12165 [BS-68], SOM: fig. S2A–F) highlight the shell colour pattern which is enhanced after the immersion in diluted commercial bleach for 72 h; this treatment causes also a whitening of the shell. No clear colour ornamentation pattern appears evident in UV and VV light photographs of the specimen of *Conus* sp. (MPUM 12163 [BS-148]; Figs. 2B, 3C), except for a faint colour pattern in the spiral part mainly observable with the 365 nm wavelength (Fig. 2B_{14a}). After the immersion of the specimen in pure commercial bleach for 72 h this spiral ornamentation becomes more pronounced and fluorescent (yellow-orange, Fig. 3C₂–C₄) and, in the middle part of the last whorl, a spiral band appears; the latter is not visible in the shell before the bleach treatment and in visible light.

Specimens photographed in visible and UV and VV light which have not experienced the bleach treatment are shown in Fig. 4. The specimen of *G. nummaria* (MPUM 12162 [ACG261-I], Fig. 4A, SOM: figs. S3, S4) under UV and VV light, besides showing very distinct muscle scars and pallial line, also reveals a lighter coloured area in the anterior part, that is light brown in visible light. A sharp boundary separates this region from the rest of the valve, which appears dark coloured in UV and VV light and whitish in visible light. A comparable situation is noted also in the silicified valve of *Vaccinites* sp. (MPUM 12167 [OMAN-I], Fig. 4B), which, when seen under UV and VV light, seems to be divided in two parts. These two regions are slightly detectable also in visible light (whitish left side, light brown right side), but UV and VV photography makes this aspect certainly clearer, defining a more coloured and brighter left side compared to the right side.

Specimens belonging to *Vichuvia lombar-doae*, *Prohalecites porroi*, and *Lariosaurus valceresii*, not treated with bleach, are shown in Fig. 5. Morphological characters of these specimens, when seen under UV and VV light, are emphasized thanks to the sharp contrast with the surrounding matrix; this is particularly evident for *Vichuvia lombar-*

doae (Fig. 5A) and *Prohalecites porroi* (Fig. 5B) which are not distinguishable on the matrix in visible light, but due to their yellow-orange fluorescence in UV and VV light, they do become very distinct in UV and VV photography. In visible light the skull of *L. valceresii* (Fig. 5C) is difficult to distinguish from the surrounding matrix, as bones and sediment have nearly the same colour; when UV and VV photographed the details of the skull become very distinct, emitting a weak fluorescence.

Discussion

Protocols

Sample preparation.—The macroinvertebrate fossil specimens analysed herein (brachiopods, bivalves, gastropods) have been selected to test the efficacy of the bleach treatment to enhance shell colour patterns in different taxa seen under UV and VV light. In the literature this procedure is often used to reveal pigment residues in the shells (Table 1), having also the advantage to be a non-destructive method for fossil specimens. Many researches applied this procedure, generally on molluscs, whereas few studies have been carried out on brachiopod shells, possibly because the colour ornamentation is rarely preserved in fossil brachiopods (Gaspard and Loubry 2017; Gaspard et al. 2019).

Our results show that the response of brachiopods, bivalves, and gastropods to different concentration and time exposure to commercial bleach is diverse and not straightforward. The use of pure or diluted commercial bleach for 3–72 h in the early Permian specimens of *Pachycyrtella omanensis* does not enhance any character or make previous colour ornamentation to appear, but slightly brighten the shells when observed in UV and VV light. This result is in agreement with the findings of Gaspard and Loubry (2017) and Gaspard et al. (2019). Although these authors decided not to immerse brachiopod shells in bleach prior to UV photography to avoid the alteration/destruction of organic matrices of the biominerals useful for other aims of their investigation, they tested this procedure in a few specimens but the results were not outstanding.

Although for brachiopod shells the bleach treatment appears to be irrelevant, this procedure applied on mollusc shells, both bivalves and gastropods, is generally successful although with different responses. As noted also in previous studies (e.g., Merle et al. 2008) bleach often whitens the

← Fig. 2. Gastropods and bivalves photographed under visible, UV, and VV light. A. Olivid gastropod *Oliva bulbosa* (Röding, 1798) from the Holocene Inqitat Khor Rori Archaeological Park, Oman. MPUM 12166 (BS-94), aboral (A₁–A₆) and oral (A₇–A₁₂) views, visible light (A₁, A₄, A₇, A₁₀), 365 nm (A₂, A₅, A₈, A₁₁) and 440 nm (A₃, A₆, A₉, A₁₂). B. Conid gastropod *Conus* sp. from the Holocene Inqitat Khor Rori Archaeological Park, Oman. MPUM 12163 (BS-148), apical (B₁₃–B₁₈), aboral (B₁–B₆), and oral (B₇–B₁₂), views, visible light (B₁, B₄, B₇, B₁₀, B₁₃, B₁₆), 365 nm (B₂, B₅, B₈, B₁₁, B₁₄, B₁₇) and 440 nm (B₃, B₆, B₉, B₁₂, B₁₅, B₁₈). C. Arcoid bivalve *Glycymeris nummaria* (Linnaeus, 1758) from the Lower Pleistocene Arda River section, Italy. MPUM 12159 (ACG204-4), left valve in external (C₁–C₆) and internal (C₇–C₁₂) views, visible light (C₁, C₄, C₇, C₁₀), 365 nm (C₂, C₅, C₈, C₁₁) and 440 nm (C₃, C₆, C₉, C₁₂). a, without treatment; b, after 72 h of immersion in 50% diluted bleach (MPUM 12166 [BS-94]) or pure bleach (MPUM 12163 [BS-148] MPUM 12159 [ACG204-4]).

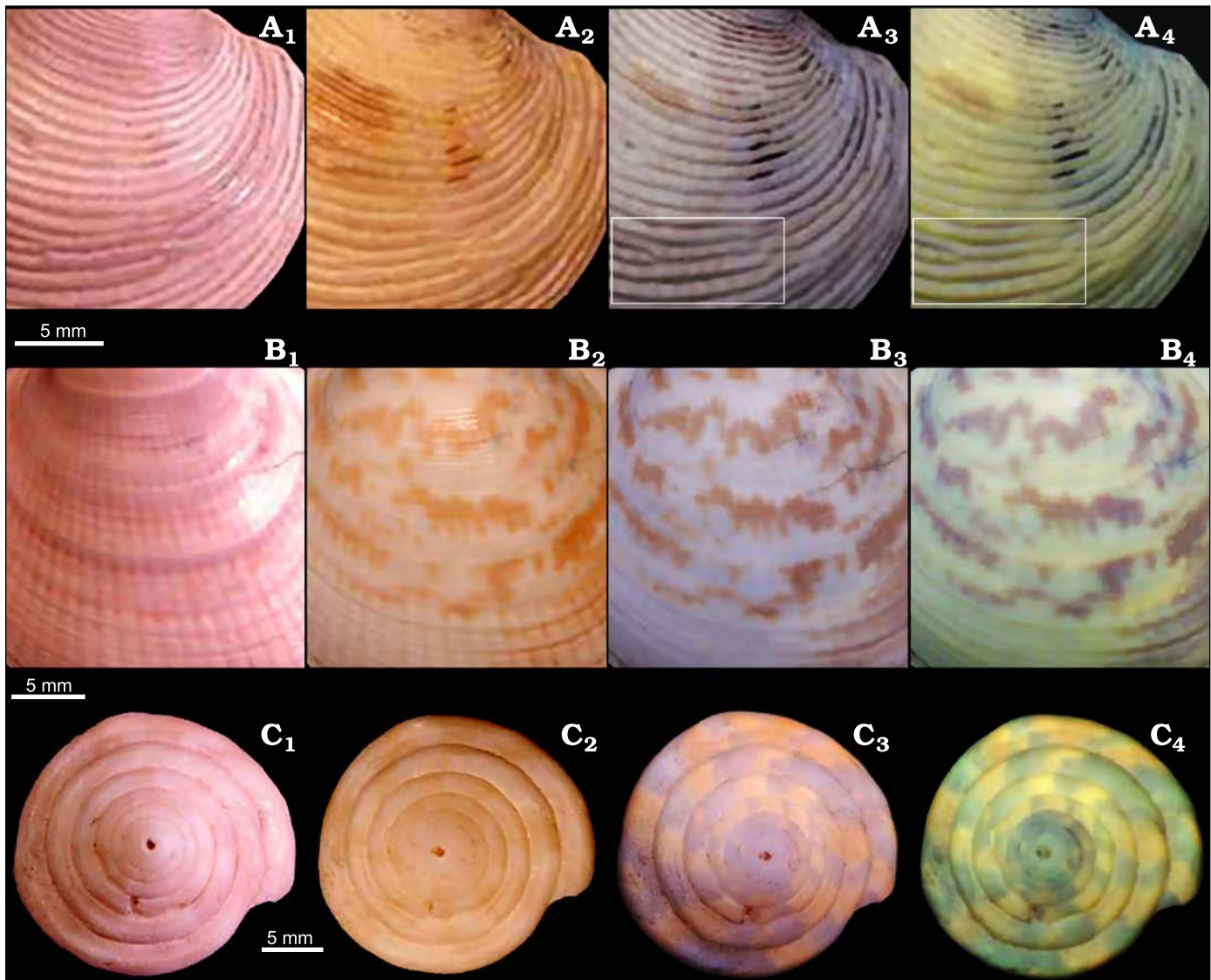


Fig. 3. Bivalves and gastropods photographed under visible, UV, and VV light. **A.** Venerid bivalve *Chamelea gallina* (Linnaeus, 1758) from the Lower Pleistocene Arda River section, Italy. MPUM 12161 (ACG204), right valve in external view. In the white rectangles is highlighted a fine zig zag colour pattern. **B.** Arcoid bivalve *Glycymeris nummaria* (Linnaeus, 1758) from the Lower Pleistocene Arda River section, Italy. MPUM 12159 (ACG204-4), left valve in external view. **C.** Conid gastropod *Conus* sp. from the Holocene Inqitat Khor Rori Archaeological Park, Oman. MPUM 12163 (BS-148) in apical view. These specimens experienced a 72 h immersion in 50% diluted bleach (MPUM 12161 [ACG204]) or pure bleach (MPUM 12159 [ACG204-4], MPUM 12163 [BS-148]). Visible light, without treatment (A₁–C₁); visible light, bleach treatment (A₂–C₂); 365 nm, bleach treatment (A₃–C₃); 440 nm, bleach treatment (A₄–C₄).

shells but at the same time it oxidises the pigments enhancing the colour pattern.

The most significant result is observable in the specimen of *Glycymeris nummaria* from the Lower Pleistocene Arda River section, which, after an immersion in commercial bleach for 72 h, reveals a distinct colour ornamentation in visible light that was not evident before the treatment (Figs. 2C_{1a}–C_{6b}, 3B). Although with lesser extent, also the specimens of *Chamelea gallina* from the Lower Pleistocene Arda River section (Figs. 1C_{1a}–C_{6b}, 3A) and of *Conus* sp. from the Holocene Khor Rori Archaeological Park in Oman (Figs. 2B, 3C) show the same response. In all these specimens the appearance of pigmented patterns is given by solely bathing

the specimens in pure or diluted commercial bleach for 72 h and it is emphasized by photographs under UV and VV light. The same phenomenon was also observed by Krueger (1974) in caenogastropods specimens. However, this behaviour has been detected only in a few of the mollusc specimens here analysed, and the factors influencing this phenomenon remain unknown.

The different stratigraphic contexts are not the trigger factor for this phenomenon, as specimens coming from different sites and ages show the same results, i.e., specimens of *Conus* sp. from the Holocene Khor Rori Archaeological Park in Oman and of *Glycymeris nummaria* and *Chamelea gallina* both from the Lower Pleistocene Arda River section

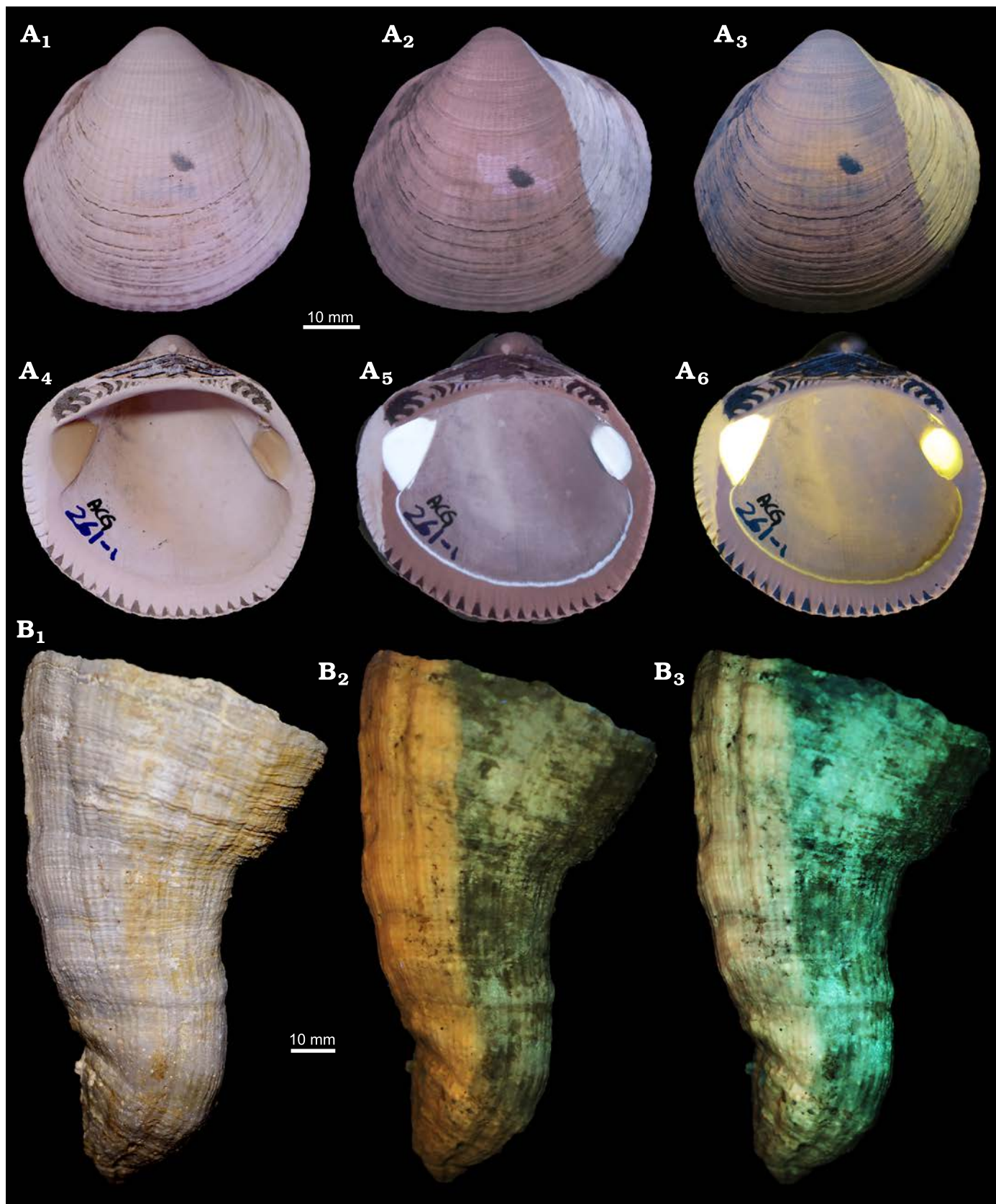


Fig. 4. Bivalves photographed under visible, UV, and VV light. **A.** Arcoïd bivalve *Glycymeris nummaria* (Linnaeus, 1758) from the Lower Pleistocene Arda River section, Italy. MPUM 12162 (ACG261-1), right valve in external (A₁–A₃) and internal (A₄–A₆) view, visible light (A₁, A₄), 365 nm (A₂, A₅) and 440 nm (A₃, A₆). **B.** Hippuritid bivalve *Vaccinites* sp. from the Upper Cretaceous Samhan Formation, Oman. MPUM 12167 (OMAN-1), conical valve, visible light (B₁), 365 nm (B₂) and 440 nm (B₃).

in Italy. Furthermore, the latter two species were sampled in different lithologies (clay/silt for *Chamelea gallina* and fine sands for *Glycymeris nummaria*) allowing to infer that, although lithology plays an important role in controlling diagenetic alteration, it is not a discriminant factor for the observed reaction. At the same time, other specimens coming from the same stratigraphic context, such as *Oliva bulbosa* from the Holocene Khor Rori Archaeological Park and *Aequipecten opercularis* from the Lower Pleistocene Arda River section, do not show the same response after the bleach treatment and no hidden colour pattern appears.

To further check if this variable response is species-specific we have exposed to the same treatment (72 h in bleach) an additional specimen of *G. nummaria* (MPUM 12157 [ACG204-A], SOM: fig. S5) coming from the same bed of the Lower Pleistocene Arda River section of the first specimen analysed (MPUM 12159 [ACG204-4]). However, only a very faint colour ornamentation appeared in this second specimen, in any case not comparable to the one emerged in the first analysed specimen, allowing to suppose that the presence vs absence of reaction (i.e., appearance of a colour pattern) is not species-specific.

The reasons of why in some specimens the treatment with bleach reveals a hidden colour pattern is currently not clear. According to Krueger (1974) this phenomenon is rare and depends on the complex chemical nature of the pigments. Possibly this reason, coupled with the taphonomic history of each specimen (e.g., diagenesis can destroy residual pigments and previous existing pattern, prolonged exposure of the shell to sunlight in the outcrop can have stronger effect than bleach) and its taxonomic position (e.g., lack of pigmentation in some species), may explain this phenomenon, which, however, needs further investigations with more specimens to be tested.

Despite that commercial bleach is readily available and inexpensive, we suggest that for brachiopods it is not essential for observing the specimens in UV and VV light, as no significant response has been observed. In the case of mollusc shells, although the responses can be different, the treatment with bleach is recommended as hidden colour patterns are revealed in most of the specimens, both in visible and UV and VV light. The majority of previously studied shells were immersed in bleach for a time interval of 12 or 24 h (Merle et al. 2008; Caze et al. 2011a, 2012, 2015; Koskeridou and Thivaïou 2012; Hendricks 2015). Here we suggest a bleach treatment lasting 24–72 h, as also indicated by Kase et al. (2008); these authors observed that the different time exposure is dependent on the state of preservation of the fossil shells. Unfortunately, it is not possible to specify which group of fossils should be treated for 24 h or 72 h. Indeed, for both bivalves and gastropods the 72 h treatment, besides allowing the reappearance of pigmented patterns, in some species (e.g., the bivalve *Chamelea gallina* and the gastropod *Oliva bulbosa*) may whiten the shells considerably (SOM: figs. S1–S5). The same phenomenon (i.e., shell whitening) is thus noted in both groups, allowing not to discern

and specify a different time exposure to bleach for one particular group. It is thus recommended to check the specimens after 24 h and, if no visible shell whitening is observed, to leave them in commercial bleach for a longer time. Aside from whitening the shells, bleach does not cause any damage to biominerals (Carriker 1979; Gaffey and Bronnimann 1993). Gaffey and Bronnimann (1993) immersed green algae and echinoid plates in 5% NaOCl for up to 11 days and no dissolution or etching was evident when looking the samples at the SEM. Indeed, sodium hypochlorite, and hydrogen peroxide, are commonly used to remove organic compounds from biogenic skeletons (e.g., Curry et al. 1991; Geiger et al. 2007; Crippa et al. 2016). On the contrary, caution has to be paid when using bleached shells for geochemical analysis, as these cleaning methods can produce moderate isotope bias or alter the trace elemental compositions (e.g., Gaffey and Bronnimann 1993; Grotoli et al. 2005; Wierzbowski 2007; Schöne et al. 2017 and references therein).

Finally, we have not observed any particular difference in using pure or 50% diluted commercial bleach (SOM: figs. S1–S5). Although in our experiments the response of the specimens under UV and VV light was not strictly affected by bleach concentration, it is possible that the use of pure bleach allows to achieve better results. Indeed, Krueger (1974) noted that the stronger the bleach, the more quickly the results are obtained.

Photography.—In addition to the bleach treatment that plays an important role in highlighting pigmented areas in the shells, the use of a proper photographic procedure is a fundamental aspect to examine fossil specimens under UV and VV light. Brachiopods, molluscs, crustaceans, fishes, and reptiles have been here photographed using two flashlights emitting two different wavelengths, 365 nm and 440 nm. Previous authors (Table 2) did not employ flashlights, but lamps diffusing the UV light. The advantage in using flashlights is that they allow to focus the beam directly on the sample detailing specific characters of a specimen. If this is very useful for small specimens, like macroinvertebrates (e.g., brachiopods or molluscs) and small-sized vertebrates, or for examining limited areas of large specimens, for large-size samples the use of flashlights does not allow to capture an overview of the entire sample; the latter would be possible only increasing the distance between the flashlight and the specimen, but the sample would be then illuminated by a less intense UV light beam similar to that of a lamp. Thus, for large size samples the choice of lamps can be more convenient. Sometimes the use of flashlights may result in overexposed photos; however, this can be easily resolved using proper camera settings when taking the pictures or with photo adjustments in post-production (e.g., brightness, contrast).

As stated above, besides the 365 nm wavelength, we have here adopted for the first time the 440 nm, which has never been used in previous studies, as it does not belong to the UV spectrum but to the visible violet. In photographing

the specimens, we have noted that characters of brachiopod shells are better emphasized with the 440 nm wavelength, whereas those of mollusc, crustacean, fish, and reptile fossils with the 365 nm; this different response will be discussed in detail in the subsequent paragraph.

Previous authors used different cameras, generally professional or semi-professional cameras (Table 2). Our experiments show that it is not necessary to employ particularly technologically advanced or expensive cameras, but it is important to have a lens able to mount the appropriate filters, and that the device can acquire images in RAW format. Also, the use of a filter capable of removing any portions of UV and IR spectra that may be recorded by the camera sensor is highly recommended. Indeed, according to Hone et al. (2010), the differences observed in the specimens viewed in UV light are enhanced considerably by an established filtering technique which is crucial for the photographic documentation. The application of different colour correction filters affixed to the lens allows a selective visualisation of peculiar fine structures by providing additional contrast. For an exhaustive comparison between photos taken with different equipment (cameras, lenses, filters, UV sources, etc.) see Eklund et al. (2018).

After capturing all the photos, the images have been colour balanced using the software “Samsung Raw Converter” and the white gypsum as reference; any other program able of processing images in RAW format can be used. The white gypsum here used is provided and tested just for this study, allowing an easy comparison among the photos of the different specimens here photographed. However, this comparison becomes difficult with third-party works. Indeed, one of the main problems is due to the absence of a clearly defined standard for colour-balance. Hendricks (2015) made adjustments to the images (white balance and levels of individual images, tone, contrast) using Adobe Photoshop CS6. This author and Kase et al. (2008) also digitally reversed in colour (using Photoshop’s invert function) the images of most fossil gastropods specimens photographed under UV light in order to reconstruct shell colouration patterns to facilitate the comparison between fossil and modern species. Hendricks (2015) stated that these reversed images do not show actual shell colours of the organism when it was alive, but this procedure is useful because differences in colour on the same shell may correspond with variability in the underlying organic molecules that are fluorescing under UV light. Here, we have preferred to keep the true appearance of the colour patterns as observed under UV light without reversing the images; the same has been done also by other authors (e.g., Caze et al. 2011a, b, 2012, 2015; Crippa and Teruzzi 2017).

Finally, it is highly recommended for pictorial quality of the resulting images to wear black gloves and cover the arms with black or dark clothing during the entire time of the photographic procedure because the human skin and some light-coloured fabrics fluoresce under UV light and this might influence the quality of the images. This is mandatory also for personal safety; gloves, long-sleeved shirt

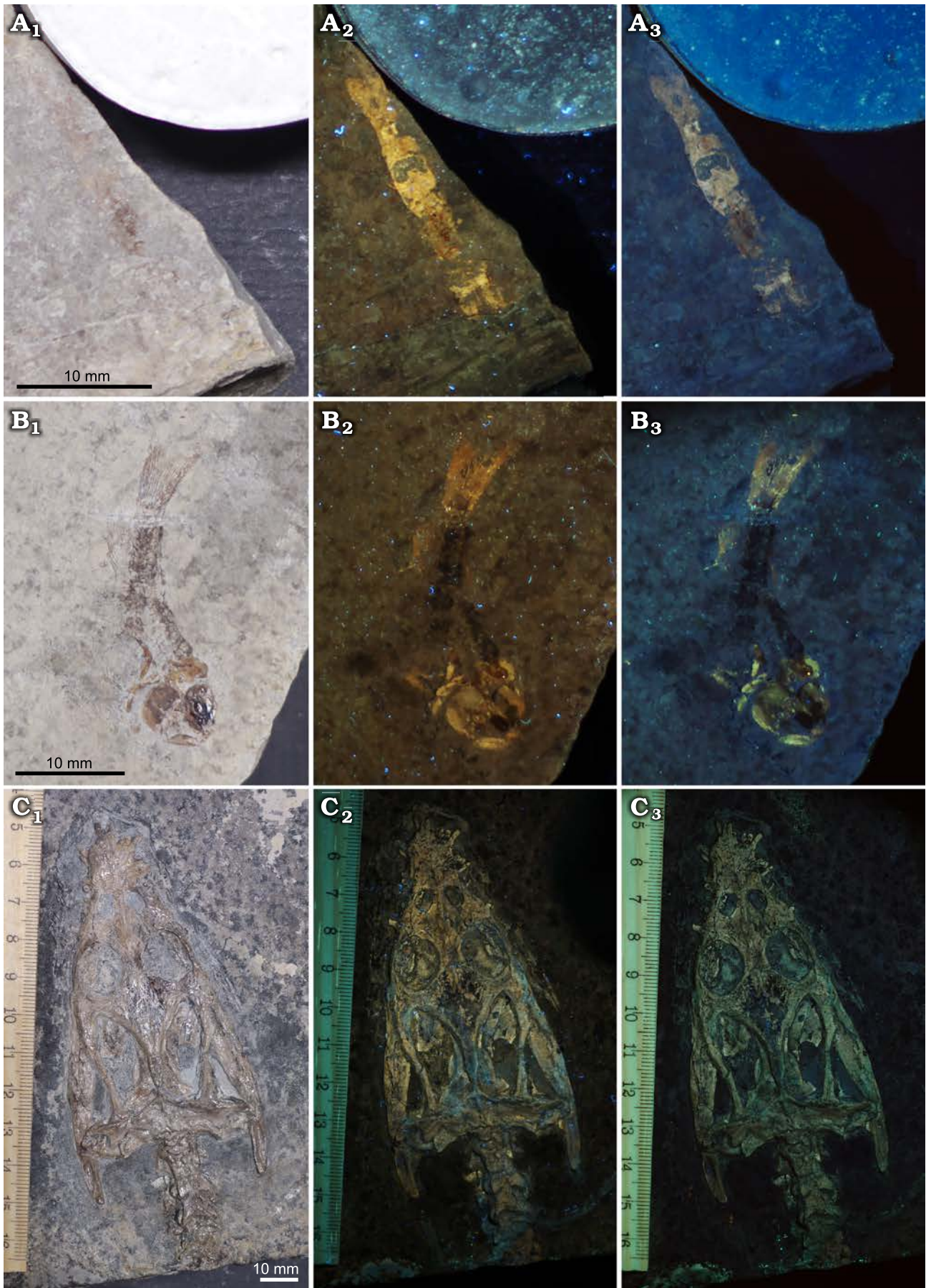
to protect the skin and glasses with UV and VV protective lenses, must be worn when taking photos under UV and VV light. Also, we recommend to leave the flashlights on only for the time necessary to capture the image in order to avoid prolonged exposure to UV and VV light.

All the photographic equipment here adopted for UV and VV photography is generally inexpensive and do not occupy a large space, being thus easily storable in a wardrobe or even a drawer and, at the same time, easily transportable.

Palaeontological information provided by UV and VV photography

The main advantage of UV and VV photography is that this technique can be applied to all the fossil groups, both invertebrate and vertebrate, having a high potential of exploration in palaeontology and no particular limitations for its application in different taxa (Table 1); also microfossils can be observed under UV and VV light simply focusing the beam directly on the microscope stage where the sample is placed.

Systematics.—Several papers deal with the application of UV photography in both invertebrate and vertebrate systematics. First of all, this technique is of great help in highlighting specimens from their matrix (e.g., Haug et al. 2009; Hone et al. 2010, 2012; Crippa and Teruzzi 2017; Eklund et al. 2018). This is particularly evident in the case of the specimens of *Vicluvia lombardoae* and *Prohalecites porroi* (Fig. 5A, B) here analysed: UV and VV light enormously increases the contrast between the specimens and the surrounding sediment highlighting morphological characters useful for the systematic description and classification; photos are brighter with the 365 nm wavelength (UV). As observed also by Hone et al. (2010), essential details of bones or soft parts can be exclusively demonstrated by UV photography as many tiny features and differences in colour and composition are not discernible in visible light or with a microscope. Indeed, the bones of the skull of the specimen *Lariosaurus valceresii* (Fig. 5C) are obscure in visible light, but well outlined under UV and VV light (brighter with the 365 nm wavelength) allowing a more accurate description of the skull morphology. The bones of *L. valceresii* emit a weak fluorescence under UV and VV light, whereas those of *Prohalecites porroi* are highly fluorescent; both are made of bioapatite. Also the crustacean *V. lombardoae* is highly fluorescent under UV and VV light because this sample is phosphatized (Larghi et al. 2020); phosphatization has been observed also in insects coming from the same site (Montagna et al. 2017). Haug et al. (2009), analysing the elemental composition of fluorescent fossil shrimp cuticles from the Upper Jurassic of southern Germany and from the Upper Cretaceous of Lebanon and of their surrounding matrix with X-ray spectroscopy, found out that fossils differed significantly from the surrounding matrix by containing 6–14% of phosphorus. According to Tischlinger and Arratia (2013) calcium phosphate, fossils with traces of organic material or



remains of uranium-bearing minerals usually show a significant fluorescence emission. Indeed, the analysed specimens of *V. lombardoae*, *Prohalecites porroi*, and *L. valceresii* are fluorescent because of the presence of phosphorus.

The nature of the biomineral plays also an important role in defining the response of brachiopod and molluscs specimens under the 365 nm and 440 nm wavelengths. As stated in the previous paragraph, brachiopod morphological characters seem to be better enhanced when samples are inspected with the 440 nm wavelength, whereas for molluscs, as for the crustacean, fish and reptile, the 365 nm wavelength seems the most effective one. The rhynchonelliform brachiopod here studied (*P. omanensis*), possesses a low magnesium calcite shell (Cusack et al. 1997; Williams and Cusack 2007), whereas bivalves and gastropods species (*Glycymeris nummaria*, *Chamelea gallina*, *Oliva bulbosa*, *Conus* sp.) have an entirely aragonitic shells (Taylor et al. 1969; Carter 1990; Tursch and Machbaete 1995; Keller et al. 2002; Rodriguez-Navarro et al. 2012; Cheli et al. 2021); *Aequipecten opercularis* represents an exception to this behaviour as this species has a shell composed by both calcite and aragonite (Taylor et al. 1969; Carter 1990). Indeed, as happens for brachiopods, characters of *A. opercularis* specimens are more defined when examined with the 440 nm wavelength. It thus seems that details of low magnesium calcite shells are better appreciable with the 440 nm wavelength, whereas those of aragonite, bioapatite and phosphatized specimens with the 365 nm. Here, we propose a combined use of both wavelengths (365 nm and 440 nm) that allows to describe in details and with a higher resolution the morphological characters of a fossil specimen, compensating the bias of using only one wavelength.

Differences in the nature of the biomineral cannot be taken into account to explain why specific areas of bivalve specimens, such as the muscle scars and the pallial line, emit fluorescence under UV and VV light. This phenomenon has never been investigated in detail and thus is not clearly understood. Bivalve muscle scars and the pallial line are always composed by aragonite (e.g., Oberling 1964; Taylor et al. 1969; Carter et al. 2012); aside from *A. opercularis* which has a shell composed by both calcium carbonate polymorphs, *Glycymeris nummaria* and *Chamelea gallina* have an entirely aragonitic shell thus there is no difference in the mineralogy of the biominerals between fluorescent and not fluorescent shell areas. What is varying between fluorescent and not fluorescent zones is the shell microstructure that may thus play a role in explaining the different observed reactions: muscle scars and the pallial line have an irregular simple prismatic microstructure (e.g., Taylor et al. 1969; Carter et al. 2012; Crippa et al. 2020b), whereas, outside these regions, shells have a crossed lamellar (*G. nummaria*;

Taylor et al. 1969; Carter 1990) or homogeneous/compound prismatic microstructure (*Chamelea gallina*; Popov 1986; Gizzi et al. 2016; Guarino et al. 2019). Different microstructures show different crystal arrangement and different elemental distribution (e.g., Masuda and Hirano 1980; Carriker et al. 1991); this is also due to the different organic contents in each microstructure (e.g., Marin et al. 2012), although the role of the organic matrix in the elemental incorporation is still not clear (Freitas et al. 2009). All these factors may cause the contrasting response of these areas when photographed under UV and VV light.

In order to distinguish and characterise biological groups and species in fossil molluscs, palaeontologists have to rely on shell morphology, but in many taxa (e.g., conid gastropods) the discriminant factor to differentiate groups at systematic levels is the colour ornamentation (Caze et al. 2011a). UV photography can be a useful tool in this respect emphasizing hidden colour patterns or making them to be revealed or fluoresce, allowing an easier identification at specific level (e.g., Merle et al. 2008; Caze et al. 2011b, 2012, 2015; Hendricks 2015). However, specimen preservation and the chemical nature of the residual pigments can affect the UV and VV results. Caze et al. (2011b, 2012, 2015) observed that the shell should not be recrystallized or decalcified, as recrystallization during diagenesis destroys the UV responsive residual pigments; some of them may still be detected in visible light in recrystallized shells, but do not emit fluorescence. However, Hendricks (2018) observed in a calcite cast questionably assigned to *Conus aemulator* Brown and Pilsbry, 1911, that a coloration pattern appears when the specimen is examined under UV light, suggesting that the replacement of aragonite with calcite is highly localised, preserving in place the fluorescing components once associated with pigmented regions. Also, pigments not always are fluorescent in UV light and this is linked to their chemical composition. For example, tetrapyrroles, as porphyrins, produce a red fluorescence under UV light, whereas melanins or melanoproteins do not fluoresce under UV light, but are very resistant in time, so they can be preserved in fossil specimens (Caze et al. 2012). In the analysed specimens different reactions have been observed: *G. nummaria* and *O. bulbosa* show a red-brown not fluorescent colour pattern, whereas *Conus* sp. exhibits a yellow-orange luminescent colour ornamentation. As observed by Hedegaard et al. (2006) pigments differ between taxa and there is no simple relationship between colour, pigment and taxon, therefore without high resolution analyses (e.g., Raman spectroscopy) it is not possible to infer or hypothesise which are the pigment types responsible for the observed colour patterns.

Taphonomy.—UV and VV photography may implement the information on the taphonomic conditions experienced by

← Fig. 5. Crustacean, fish, and reptile specimens from the Middle Triassic Meride Limestone, Italy photographed under visible, UV, and VV light. **A.** Lophogastrid crustacean *Vichuvia lombardoae* Larghi, Tintori, Basso, Danini, and Felber, 2020; MPUM 12168. **B.** Actinopterygian fish *Prohalecites porroi* (Bellotti, 1857); MPUM 12169. **C.** Sauropterygian reptile *Lariosaurus valceresii* Tintori and Renesto, 1990; MCSNIO 701, skull. Visible light (A₁–C₁), 365 nm (A₂–C₂), and 440 nm (A₃–C₃).

fossil specimens, i.e. of all the events occurring from the death of an organism to its discovery as a fossil within a sedimentary rock; thus also Recent processes (e.g., erosion, quarrying activities, etc.) that modify the conditions of a specimen before its discovery can be considered part of the taphonomic process. An example of that is given by the specimens of *Glycymeris nummaria* (MPUM 12162 [ACG261-1]) and *Vaccinites* sp. (Fig. 4); when seen under UV and VV light they show a sharp subdivision of the shells in two distinct regions, that are made more evident by the colour contrast. This behaviour is independent from the preservation conditions of the specimens or from their mineralogy, as *G. nummaria* is a well preserved aragonitic shell whereas *Vaccinites* sp. is a silicified specimen (Philip and Platel 1995; GC and SM, personal observations). According to Krueger (1974) and Hendricks (2015), which observed in their specimens a similar phenomenon, the development of these two distinct regions is due to the burial position of the specimens in the outcrop prior to collection. Hendricks (2015) noted in one fossil specimen of *Conus humerosus* Pilsbry, 1921, that the part of the shell buried in the sediment shows a colour pattern in visible light, that is not observable in the shell part exposed to sunlight (and thus oxidised); however, under UV and VV light, the same colour pattern appears also on this latter part. Indeed, oxidation, caused either by a natural and prolonged exposure of shells to sunlight, or artificially by immersing the specimens in bleach for different time intervals, plays a role in causing formerly pigmented areas of fossil shells to be fluorescent under UV light though the reason is not currently understood (Hendricks 2015). In the specimens here analysed no colour pattern is revealed but a sharp division is evident. We can infer that in both *Glycymeris nummaria* and *Vaccinites* sp. the part of the specimens buried in the sediment appears not coloured under UV and VV light, whereas the other part, coloured in UV and VV, is the one that was exposed to sunlight. However, it is not possible to hypothesise when the sunlight exposure occurred in the past and which are the processes that caused it (natural or anthropogenic). This phenomenon, besides providing useful information for reconstructing the taphonomic history, may also explain why not all the specimens forming a thanatocoenosis show the same state of residual colour (Gaspard and Loubry 2017). It may also explain the different response of the two *G. nummaria* specimens coming from the same bed of the Arda River section in Italy (MPUM 12157 [ACG204-A], MPUM 12159 [ACG204-4]) and why only one of the two reveals a hidden colour pattern after the immersion in bleach (see also first paragraph of the Discussion).

Conclusions

In the present study different taxa (brachiopods, bivalves, gastropods, crustaceans, fishes, and reptiles) coming from different localities (Oman, Italy) and having different ages (Permian, Triassic, Cretaceous, Pleistocene, and Holocene)

and biominerals (calcite, aragonite, bioapatite, and silicified and phosphatized specimens) have been examined in order (i) to establish a protocol for observing fossil specimens under two different wavelengths: the 365 nm UV light and the 440 nm, belonging to the visible violet spectrum, (ii) to offer a synthesis of the available information in Tables 1 and 2 and (iii) to better understand which kind of information we can derive from UV and VV photography. The main outcomes are:

- Bleach treatment is not necessary for calcite brachiopods, whereas it is suggested for aragonite bivalve and gastropod specimens; in particular an immersion in pure commercial bleach for 24 to 72 h is advised.
- Specimens should be photographed in visible light and then with both the 365 nm and 440 nm wavelengths in a dark room using a camera mounted on a tripod, equipped with a fixed-focus lens and appropriate UV-IR cut and yellow filters; a white reference is necessary for white balancing in photo post-production. We suggest the use of flashlights as the main source of UV and VV light (365 nm and 440 nm) as the light beam can be focused directly on the characters to study. This equipment is not expensive and it is easily storable in a small place. A safety equipment (gloves, UV and VV protective lenses, etc.) is mandatory when taking the photos.
- UV and VV photography can be an important tool in systematics, but also for functional morphology or biological related purposes, as only with this technique is possible to detect characters invisible in visible light. Indeed, it allows to emphasize specimens from the surrounding matrix and it accentuates morphological characters (in all taxa) and colour patterns (in molluscs).
- Morphological characters of low magnesium calcite shells (brachiopods) are better emphasized with the 440 nm wavelength, whereas those of aragonite, bioapatite and phosphatized specimens (molluscs, crustacean, fish, reptile) with the 365 nm.
- UV and VV light technique is useful for reconstructing the conditions and processes experienced by a fossil specimen, as for instance it allows to discriminate between regions of fossil specimen included in the sediment and those exposed to sunlight.
- The biomineralogy and the microstructure play an important role in defining the different responses of fossil specimens under UV and VV light, whereas the stratigraphic context mainly affects the specimen preservation, and consequently that of pigments. Each shell microstructure has a different crystal arrangement and elemental distribution that may affect the elemental incorporation into the shell, thus producing different reactions under UV and VV light.

Although the response of fossil specimens in UV and VV light is not always well understood, this technique can be a very useful tool in palaeontology, as it has no particular limitations for its application in invertebrate or vertebrate specimens and in macro- or microfossils.

Acknowledgements

We warmly thank Lucia Angiolini (University of Milan, Italy) for the critical reading on a first version of the manuscript and for providing the brachiopod specimens here analysed. Cristina Lombardo (University of Milan, Italy) is deeply thanked for helping us with the analysis of the specimens of the Meride Formation. Davide Manzini (MADAtec s.r.l., Pessano con Bornago, Italy) is acknowledged for supporting us in the use of UV flashlights. Silvia Lischi (University of Pisa, Italy) and Mauro Cremaschi (University of Milan, Italy) are thanked for supplying the gastropod specimens from the Khor Rori Archaeological Park. Gaia Crippa acknowledges financial support of the 2017 Italian Ministry PRIN RX9XXY Project “Biota resilience to global change: biomineralization of planktic and benthic calcifiers in the past, present and future” to E. Erba. Jonathan Hendricks (Paleontological Research Institution, Ithaca, USA) and an anonymous reviewer are thanked for their constructive comments which improve the quality of the manuscript.

References

- Angiolini, L. 2001. New syringothyridid genus (Spiriferinida, Brachiopoda) from the Early Permian of Interior Oman. *Rivista Italiana di Paleontologia e Stratigrafia* 107: 125–130.
- Angiolini, L. 2007. Quantitative palaeoecology in the *Pachycyrtella* Bed, Early Permian of Interior Oman. *Palaeoworld* 16: 233–245.
- Barnard, W. and Waal, D. de 2006. Raman investigation of pigmentary molecules in the molluscan biogenic matrix. *Journal of Raman Spectroscopy* 37: 342–352.
- Bellotti, C. 1857. Descrizione di alcune nuove specie di pesci fossili di Perledo e di altre località lombarde. In: A. Stoppani (ed.), *Studi geologici e paleontologici sulla Lombardia*, 419–438. Turati, Milano.
- Brown, A.P. and Pilsbry, H.A. 1911. Fauna of the Gatun formation, Isthmus of Panama. *Proceedings of the Academy of Natural Sciences of Philadelphia* 63: 336–373.
- Carriker, M.R. 1979. Ultrastructural effect of cleaning molluscan shell with sodium-hypochlorite (Clorox). *Nautilus* 93: 47–50.
- Carriker, M.R., Swann, C.P., Prezant, R.S., and Counts, C.L. 1991. Chemical elements in the aragonitic and calcitic microstructural groups of shell of the oyster *Crassostrea virginica*: a proton probe study. *Marine Biology* 109: 287–297.
- Carter, J.G. 1990. *Skeletal Biomineralization: Patterns, Processes and Evolutionary Trends*. 832 pp. Van Nostrand Reinhold, New York.
- Carter, J.G., Harries, P.J., Malchus, N., Sartori, A.F., Anderson, L.C., Bieler, R., Bogan, A.E., Coan, E.V., Cope, J.C.W., Cragg, S.M., García-March, J.R., Hylleberg, J., Kelley, P., Kleemann, K., Kříž, J., McRoberts, C., Mikkelsen, P.M., Pojeta Jr, J., Tëmkin, I., Yancey, T. et al. 2012. Illustrated glossary of the Bivalvia. In: *Treatise Online 48, Part N, Revised, Volume 1, Chapter 31*. 209 pp. Paleontological Institute, The University of Kansas, Lawrence.
- Caze, B., Merle, D., Le Meur, M., Pacaud, J.-M., Ledon, D., and Saint Martin, J.-P. 2011a. Taxonomic implications of the residual colour patterns of ampullinid gastropods and their contribution to the discrimination from naticids. *Acta Paleontologica Polonica* 56: 329–347.
- Caze, B., Merle, D., Saint Martin, J.P., and Pacaud, J.M. 2011b. Contribution of residual colour patterns to the species characterization of Caenozoic molluscs (Gastropoda, Bivalvia). *Comptes Rendus Palevol* 10: 171–179.
- Caze, B., Merle, D., Saint Martin, J.P., and Pacaud, J.M. 2012. Les mollusques éocènes se dévoilent sous ultraviolets. *Les coquillages de l'Éocène du Bassin parisien, Fossiles, hors-série III*: 15–56.
- Caze, B., Merle, D., and Schneider, S. 2015. UV Light reveals the diversity of Jurassic shell colour patterns: examples from the Cordebugle Lagerstätte (Calvados, France). *PLoS ONE* 10 (6): e0126745.
- Cheli, A., Mancuso, A., Azzarone, M., Fermani, S., Kaandorp, J., Marin, F., Montroni, D., Polishchuk, I., Prada, F., Stagioni, M., Valdre', G., Pokroy, B., Falini, G., Goffredo, S., and Scarponi, D. 2021. Climate variation during the Holocene influenced the skeletal properties of *Chamelea gallina* shells in the North Adriatic Sea (Italy). *PLoS One* 16 (3): e0247590.
- Comfort, A. 1951. The pigmentation of molluscan shells. *Biological Reviews* 26: 285–301.
- Corbacho, J. and Sendino, C. 2012. Fossil fakes and their recognition. *Deposits Magazine* 30: 35–40.
- Crippa, G., Baucon, A., Felletti, F., Raineri, G., and Scarponi, D. 2018. A multidisciplinary study of ecosystem evolution through early Pleistocene climate change from the marine Arda River section, Italy. *Quaternary Research* 89: 533–562.
- Crippa, G., Felletti, F., Francou, C., Marini, M., Raineri, G., Taddei Ruggiero, E., and Scarponi, D. 2020a. Palaeoclimatic and palaeoenvironmental evolution of the Lower Pleistocene Arda River succession. *Geological Field Trips and Maps* 12 (1.2): 1–41.
- Crippa, G., Griesshaber, E., Checa, A.G., Harper, E.M., Roda, M.S., and Schmahl, W.W. 2020b. Orientation patterns of aragonitic crossed-lamellar, fibrous prismatic and myostracal microstructures of modern *Glycymeris* shells. *Journal of Structural Biology* 212 (3): 107653.
- Crippa, G., Ye, F., Malinverno, C., and Rizzi, A. 2016. Which is the best method to prepare invertebrate shells for SEM analysis? Testing different techniques on recent and fossil brachiopods. *Bollettino della Società Paleontologica Italiana* 55: 111–125.
- Crippa, L.M. and Teruzzi, G. 2017. Fossili in luce UV. *Natura. Rivista Di Scienze Naturali* 107: 1–32.
- Curry, G.B., Cusack, M., Walton, D., Endo, K., Clegg, H., Abbott, G., and Armstrong, H. 1991. Biogeochemistry of brachiopod intracrystalline molecules. *Philosophical Transactions of the Royal Society of London B: Biological Sciences* 333: 359–366.
- Cusack, M., Walton, D., and Curry, G.B. 1997. Shell biochemistry. In: R.L. Kaesler (ed.), *Treatise on Invertebrate Paleontology. Part H. Brachiopoda (Revised), Vol. 1*, 243–266. Geological Society of America and University of Kansas Press, Boulder, Colorado and Lawrence, Kansas.
- Eklund, M.J., Aase, A.K., and Bell, C.J. 2018. Progressive photonics: methods and applications of sequential imaging using visible and non-visible spectra to enhance data-yield and facilitate forensic interpretation of fossils. *Journal of Paleontological Techniques* 20: 1–36.
- Freitas, P.S., Clarke, L.J., Kennedy, H., and Richardson, C.A. 2009. Ion microprobe assessment of the heterogeneity of Mg/Ca, Sr/Ca and Mn/Ca ratios in *Pecten maximus* and *Mytilus edulis* (Bivalvia) shell calcite precipitated at constant temperature. *Biogeosciences* 6: 1209–1227.
- Gaffey, S.J. and Bronnimann, C.E. 1993. Effects of bleaching in organic and mineral phases in biogenic carbonates. *Journal of Sedimentary Petrology* 63: 752–754.
- Gaspard, D. and Loubry, P. 2017. A brachiopod shell show during the middle Cenomanian in the stratotype area (France)—exceptional residual colour pattern. *Annales de Paléontologie* 103: 81–85.
- Gaspard, D., Paris, C., Loubry, P., and Luquet, G. 2019. Raman investigation of the pigment families in recent and fossil brachiopod shells. *Spectrochimica Acta Part A: Molecular and Biomolecular Spectroscopy* 208: 73–84.
- Geiger, D.L., Marshall, B.A., Ponder, W.F., Sasaki, T., and Warén, A. 2007. Techniques for collecting, handling, preparing, storing and examining small molluscan specimens. *Molluscan Research* 27: 1–50.
- Gizzi, F., Caccia, M.G., Simoncini, G.A., Mancuso, A., Reggi, M., Fermani, S., Brizi, L., Fantazzini, P., Stagioni, M., Falini, G., Piccinetti, C., and Goffredo, S. 2016. Shell properties of commercial clam *Chamelea gallina* are influenced by temperature and solar radiation along a wide latitudinal gradient. *Scientific Reports* 6: 36420.
- Górka, M. 2008. Shell colour pattern in two fossil helicid snails, *Tropidomphalus incrassatus* (Klein, 1853) and *Cepaea sylvestrina gottschi* Wenz, 1919, from the Middle Miocene of Poland. *Acta Geologica Polonica* 58: 105–111.
- Grottoli, A.G., Rodrigues, L.J., Matthews, K.A., Palardy, J.E., and Gibb, O.T. 2005. Pre-treatment effects on coral skeletal $\delta^{13}\text{C}$ and $\delta^{18}\text{O}$. *Chemical Geology* 221: 225–242.
- Guarino, R., Goffredo, S., Falini, G., and Pugno, N.M. 2019. Mechanical properties of *Chamelea gallina* shells at different latitudes. *Journal of the Mechanical Behavior of Biomedical Materials* 94: 155–163.

- Harper, D.A.T., Popov, L.E., and Holmer, L.E. 2017. Brachiopods: origin and early history. *Palaeontology* 60: 609–631.
- Haug, C., Haug, J.T., Waloszek, D., Maas, A., Frattigiani, R., and Liebau, S. 2009. New methods to document fossils from lithographic limestones of southern Germany and Lebanon. *Palaeontologia Electronica* 12: 12.3.6T.
- Hedegaard, C., Bardeau, J.F., and Chateigner, D. 2006. Molluscan shell pigments: an in situ resonance Raman study. *Journal of Molluscan Studies* 72: 157–162.
- Hendricks, J.R. 2015. Glowing seashells: diversity of fossilized coloration patterns on coral reef-associated cone snail (Gastropoda: Conidae) shells from the Neogene of the Dominican Republic. *PLoS One* 10 (4): e0120924.
- Hendricks, J.R. 2018. Diversity and preserved shell coloration patterns of Miocene Conidae (Neogastropoda) from an exposure of the Gatun Formation, Colón Province, Panama. *Journal of Paleontology* 92: 804–837.
- Hoerle, S.E. 1976. The genus *Conus* (Mollusca: Gastropoda) from the Alum Bluff Group of northwestern Florida. *Tulane Studies in Geology and Paleontology* 12: 1–32.
- Hone, D.W., Tischlinger, H., Frey, E., and Röper, M. 2012. A new non-pterodactyloid pterosaur from the Late Jurassic of Southern Germany. *PLoS One* 7 (7): e39312.
- Hone, D.W., Tischlinger, H., Xu, X., and Zhang, F. 2010. The extent of the preserved feathers on the four-winged dinosaur *Microraptor gui* under ultraviolet light. *PLoS One* 5 (2): e9223.
- Kase, T., Kitao, F., Aguilar, Y.M., Kurihara, Y., and Pandita, H. 2008. Reconstruction of color markings in *Vicarya*, a Miocene potamidid gastropod (Mollusca) from SE Asia and Japan. *Paleontological Research* 12: 345–353.
- Keller, N., Del Piero, D., and Longinelli, A. 2002. Isotopic composition, growth rates and biological behaviour of *Chamelea gallina* and *Callista chione* from the Bay of Trieste (Italy). *Marine Biology* 140: 9–15.
- Koskeridou, E. and Thivaoui, D. 2012. Problematic species: Color patterns revealed by UV light as a character for systematics in mollusc fossils—an example from the Hellenic region. In: *Proceedings of the 10th Symposium on Oceanography & Fisheries, 7–11 May 2012 Athens, Greece*, 15.
- Krueger, K.K. 1974. The use of ultraviolet light in the study of fossil shells. *Curator* 17: 36–49.
- Larghi, C., Tintori, A., Basso, D., Danini, G., and Felber, M. 2020. A new Ladinian (Middle Triassic) mysidacean shrimp (Crustacea, Lophogastrida) from northern Italy and southern Switzerland. *Journal of Paleontology* 94: 291–303.
- Lindgren, J., Caldwell, M.W., Konishi, T., and Chiappe, L.M. 2010. Convergent evolution in aquatic tetrapods: insights from an exceptional fossil mosasaur. *PLoS One* 5 (8): e11998.
- Linnaeus, C. 1758. *Systema Naturae per Regna tria naturae, secundum classes, ordines, genera, species cum characteribus, differentiis, synonymis, locis*. 824 pp. Editio decima, reformata. Tomus 1, Laurentii Salvii, Holmiae.
- Lischi, S. 2016. *Al Hamr Al-Sharqiya, Preliminary Report. IMTO—Italian Mission to Oman. September–December 2016 (IQM16B)*. 68 pp. University of Pisa, Pisa.
- Lombardo, C., Tintori, A., and Tona, D. 2012. A new species of *Sangioioichthys* (Actinopterygii, Semionotiformes) from the Kalkschieferzone of Monte San Giorgio (Middle Triassic; Meride, Canton Ticino, Switzerland). *Bollettino della Società Paleontologica Italiana* 51: 203–212.
- Marin, F., Le Roy, N., and Marie, B. 2012. The formation and mineralization of mollusk shell. *Frontiers in Bioscience* S4: 1099–1125.
- Masuda, F. and Hirano, M. 1980. Chemical composition of some modern marine pelecypod. *Science Reports of the Institute of Geoscience, University of Tsukuba: Geological Sciences* 1: 163–177.
- Merle, D. 2003. First record of coloured patterns in Palaeogene Muricidae (Mollusca, Gastropoda). *Annales de Paléontologie* 89: 191–203.
- Merle, D., Pacaud, J. M., Kriloff, A., and Loubry, P. 2008. Les motifs colorés résiduels des coquilles lutétiennes du bassin de Paris. In: D. Merle (ed.), *Stratotype Lutétien*, 182–227. Muséum national d'Histoire naturelle, Paris; Biotop, Mèze; BRGM, Orléans (Patrimoine géologique).
- Montagna, M., Haug, J.T., Strada, L., Haug, C., Felber, M., and Tintori, A. 2017. Central nervous system and muscular bundles preserved in a 240 million year old giant bristletail (Archaeognatha: Machilidae). *Scientific Reports* 7: 46016.
- Oberling, J.J. 1964. Observations on some structural features of the pelecypod shell. *Mitteilungen der Naturforschenden Gesellschaft in Bern* 20: 1–60.
- Olsson, A.A. 1967. *Some Tertiary mollusks from south Florida and the Caribbean*. 61 pp. Paleontological Research Institution, Ithaca.
- Philip, J.M. and Platel, J.P. 1995. Stratigraphy and rudist biozonation of the Campanian and the Maastrichtian of Eastern Oman. *Revista Mexicana de Ciencias Geológicas* 12: 257–266.
- Pilsbry, H.A. 1921. Revision of W.M. Gabb's Tertiary Mollusca of Santo Domingo. *Proceedings of the Academy of Natural Sciences of Philadelphia* 73: 305–435.
- Pitt, W.D. and Pitt, L.J. 1993. Ultra-violet light as a useful tool for identifying fossil mollusks, with examples from the Gatun Formation, Panama. *Tulane Studies in Geology and Paleontology* 26: 1–13.
- Popov, S.V. 1986. Composite prismatic structure in bivalve shell. *Acta Palaeontologica Polonica* 31: 3–26.
- Renesto, S., Pareo, M., and Lombardo, C. 2004. A new specimen of the sauropterygian reptile *Lariosaurus* from the Kalkschieferzone (Uppermost Ladinian) of Valceresio (Varese, N Italy). *Neues Jahrbuch für Geologie und Paläontologie-Monatshefte* 2004 (6): 351–369.
- Riquelme, F., Ruvalcaba-Sil, J.L., and Alvarado-Ortega, J. 2009. Palaeometry: Non-destructive analysis of fossil materials. *Boletín de la Sociedad Geológica Mexicana* 61: 177–183.
- Röding, P.F. 1798. *Museum Boltenianum sive Catalogus cimeliorum e tribus regnis naturæ quæ olim collegerat Joa. Fried. Bolten, M. D. p. d. per XL. annos proto physicus Hamburgensis. Pars secunda continens Conchylia sive Testacea univalvia, bivalvia & multivalvia*. viii, 199 pp. Trapp, Hamburg.
- Rodriguez-Navarro, A.B., Checa, A., Willinger, M.G., Bolmaro, R., and Bonarski, J. 2012. Crystallographic relationships in the crossed lamellar microstructure of the shell of the gastropod *Conus marmoreus*. *Acta Biomaterialia* 8: 830–835.
- Schöne, B.R., Schmitt, K., and Maus, M. 2017. Effects of sample pretreatment and external contamination on bivalve shell and Carrara marble $\delta^{18}\text{O}$ and $\delta^{13}\text{C}$ signatures. *Palaeogeography, Palaeoclimatology, Palaeoecology* 484: 22–32.
- Simonpietri, G., Philip, J., and Platel, J.P. 1998. Etude statistique des espèces de *Vaccinites* (Hippuritacea, Hippuritidae) du Campanien du Sultanat d'Oman. *Geobios Mémoire Spéciale* 22: 313–329.
- Taylor, J.D., Kennedy, W.J., and Hall, A. 1969. The shell structure and mineralogy of the Bivalvia: introduction, Nuculacea-Trigonacea. *Bulletin of the British Museum of Natural History, Zoology* 3: 1–125.
- Tintori, A. 1990. The Actinopterygian fish *Prohalecites* from the Triassic of northern Italy. *Palaeontology* 33: 155–174.
- Tintori, A. and Renesto, S. 1990. A new *Lariosaurus* from the Kalkschieferzone (Uppermost Ladinian) of Valceresio (Varese, Northern Italy). *Bollettino della Società Paleontologica Italiana* 29: 309–319.
- Tischlinger, H. and Arratia, G. 2013. Ultraviolet light as a tool for investigating Mesozoic fishes, with a focus on the ichthyofauna of the Solnhofen archipelago. In: G. Arratia, H.-P. Schultze, and M.V.H. Wilson (eds.), *Mesozoic Fishes 5—Global Diversity and Evolution*, 549–560. Pfeil, München.
- Tursch, B. and Machbaete, Y. 1995. The microstructure of the shell in the genus *Oliva* (Studies on Olividae 24). *Apex* 10: 61–78.
- Vokes, H.E. and Vokes, E.H. 1968. Variation in the genus *Orthaulax* (Mollusca: gastropoda). *Tulane studies in Geology and Paleontology* 6: 71–79.
- Williams, S.T. 2017. Molluscan shell colour. *Biological Reviews* 92: 1039–1058.
- Williams, A. and Cusack, M. 2007. Chemostructural diversity of the brachiopod shell. In: R.L. Kaesler (ed.) *Treatise on Invertebrate Paleontology, Part H. Brachiopoda (Revised), Vol. 6 Supplement*, 2396–2521. Geological Society of America and University of Kansas Press, Boulder, Colorado and Lawrence, Kansas.
- Wierzbowski, H. 2007. Effects of pre-treatments and organic matter on oxygen and carbon isotope analyses of skeletal and inorganic calcium carbonate. *International Journal of Mass Spectrometry* 268: 16–29.